QUANTUM GASES

Generalized hydrodynamics in strongly interacting 1D Bose gases

Neel Malvania[1]†, Yicheng Zhang[1]†, Yuan Le[1], Jerome Dubail[2], Marcos Rigol[1], David S. Weiss[1]*

The dynamics of strongly interacting many-body quantum systems are notoriously complex and difficult to simulate. A recently proposed theory called generalized hydrodynamics (GHD) promises to efficiently accomplish such simulations for nearly integrable systems. We test GHD with bundles of ultracold one-dimensional (1D) Bose gases by performing large trap quenches in both the strong and intermediate coupling regimes. We find that theory and experiment agree well over dozens of trap oscillations, for average dimensionless coupling strengths that range from 0.3 to 9.3. Our results show that GHD can accurately describe the quantum dynamics of a 1D nearly integrable experimental system even when particle numbers are low and density changes are large and fast.

In interacting many-body quantum systems, such as electrons in a metal, the low-energy properties can often be described to a good approximation in terms of quasiparticles that travel almost freely and have a finite lifetime. In integrable systems, quasiparticles provide an exact description and live forever. They allow the efficient computation of the entire energy spectrum (*1*) and simplify the study of quantum dynamics (*2*). When there is weak integrability breaking, the quasiparticle picture remains useful at all energies. In many situations, a theory called generalized hydrodynamics (GHD) (*3*, *4*) drastically simplifies the study of dynamics by focusing on the evolution of the momenta of the quasiparticles, the rapidities (*5*).

GHD consists of coupled hydrodynamic equations that are based on two assumptions (*3*, *6*). First, the system is viewed as a continuum of fluid cells, each of which is spatially homogeneous, integrable, and contains many particles. Second, the time variation of local quantities is slow enough that each fluid cell is locally equilibrated to a generalized Gibbs ensemble (GGE) parameterized by its distribution of rapidities (*7*). Experimentally testing GHD is tantamount to determining how robust these two assumptions are in real quantum dynamical systems. GHD was recently tested experimentally for relatively hot, weakly interacting atoms (*8*). In this study, we use ultracold strongly and intermediately coupled atoms to study the quantum regime, which is characterized by strong entanglement and complex correlations among particles. We show that GHD describes the experimental results even when there are few particles (~10) and when there are rapid changes in the nature of the quasiparticles.

In our experiments and GHD simulations, we suddenly ramp up the axial trapping potential around a bundle of ultracold one-dimensional (1D) Bose gases and follow the evolution of the rapidity distribution as the gases successively collapse into the trap center and rebound (Fig. 1A). Our 1D Bose gases are initially close to their ground states, so they can each be described as a Fermi sea for quasiparticles (*9*). For a short time after the trap quench, they remain locally close to a zero-temperature Fermi-sea state. Such a situation could have been described before the advent of GHD using a hydrodynamic approach (*10*, *11*). However, GHD predicts (*12*, *13*) the eventual local formation of states with multiple Fermi seas (*14*), illustrated in Fig. 1, B and C, which shows an example of phase space evolution in the first two cycles after one of our trap quenches. Such local states cannot be modeled with the hydrodynamic methods that preceded GHD. The quantum dynamics considered here are extremely challenging for any other computational approach, except when dealing with few particles and short times or in the limiting cases of very weak or very strong interactions (*11*, *15*).

To create a bundle of ultracold 1D gases from a ^{87}Rb Bose-Einstein condensate confined by a 55-μm beam waist red-detuned crossed dipole trap, we slowly turn on a 2D blue-detuned optical lattice until it is $40E_r$ deep, where $E_r = \hbar^2k^2/(2m) = 2.55 \times 10^{-30}$ J is the recoil energy defined by the lattice light wavevector, $k = 2\pi/(772\ \text{nm})$, $\hbar$ is the reduced Planck's constant, and m is the atom mass (*16*). We use two different initial conditions to study gases that are initially either intermediately or strongly 1D coupled, as characterized by the dimensionless parameter $\gamma = 4.44/n_{1D}$, where n_{1D} is the local 1D density in units of inverse micrometers (*17*). To start with an intermediate (strong) weighted average of γ, $\bar{\gamma}_0 = 1.4$ (9.3), we use ~3×10^5 (~1×10^5) atoms in a $9.4E_r$ ($0.56E_r$) crossed dipole trap, so the 2D distribution of 1D gases extends across a 17-μm (22-μm) radius (figs. S2 and S3). These radii are much smaller than the 2D lattice beam waists of 420 μm, so the transverse confinement for each 1D gas is about the same. The axial trap depths, however, vary across the 1D gases by up to 14% (27%).

We measure rapidity distributions by first shutting off the axial trapping only and letting the atoms expand in 1D in a nearly flat axial potential until the momentum distributions have evolved into the rapidity distributions (*5*, *17*). Then we turn off the 2D lattice and

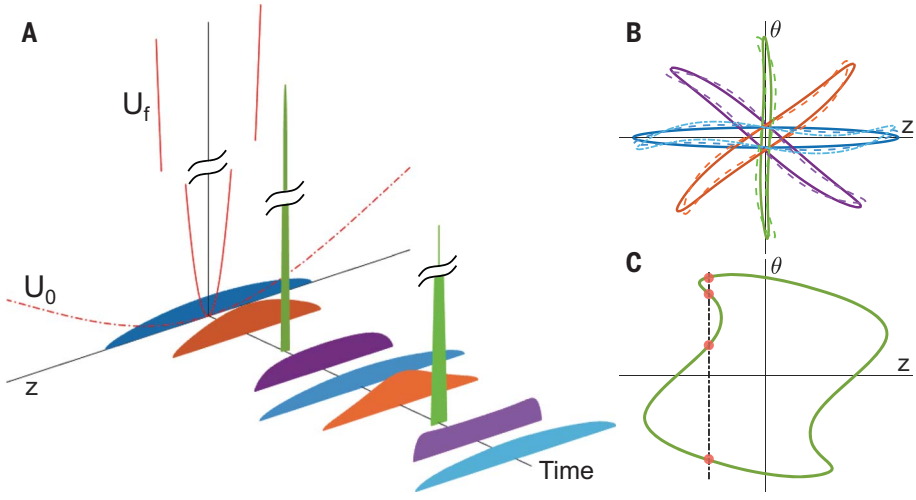

Fig. 1. GHD theory after a 100-fold trap quench. (**A**) Spatial evolution of the initially strongly coupled central 1D gas. At time $t = 0$, the trap depth, U, is increased by a factor of 100 (from the dot-dashed to the solid red lines). The colored curves are the calculated atomic density distributions at various times as the cloud collapses and expands twice. (**B**) The evolution in position (z)–rapidity (θ) space. The colors correspond to the curves in (A), with the solid lines showing the first cycle and the dashed lines showing the second cycle. (**C**) A spatially magnified view of the half-period curve in (B) (see also fig. S1). The two segments of the dashed line inside the contour depict two Fermi seas, the smaller one of which develops during the time evolution. Once a second Fermi sea forms, no existing hydrodynamic theory other than GHD can model the evolution.

[1]Department of Physics, The Pennsylvania State University, University Park, PA 16802, USA. [2]Université de Lorraine, CNRS, LPCT, F-54000 Nancy, France.
*Corresponding author. Email: dsweiss@phys.psu.edu
†These authors contributed equally to this work.

measure the rapidity distributions via time of flight. Our previous dynamical fermionization measurement (*5*) validated this momentum-to-rapidity mapping with parameters very close to our $\bar{\gamma}_0 = 9.3$ initial condition. Because all the other initial cloud lengths are smaller, which allows for relatively more expansion in the flat potential, the mappings in this work are at least as good. We also measure momentum distributions by first suddenly turning off all the light traps. As the atoms rapidly expand transversely, atom interactions decrease rapidly and substantially (*5*). The integrated axial spatial distributions after a time of flight reflect the 1D momentum distribution at the shutoff time. We adjust the times of flight for different measurements to maximize sensitivity and rescale the spatial distributions by the time of flight to obtain the momentum distributions.

Figure 2A shows the evolution of the rapidity distribution starting from $\bar{\gamma}_0 = 1.4$ after a quench to a ten-times-deeper trap. Our quenches are small enough to ensure that two atoms never have enough energy to get transversely excited in a collision, so the system remains 1D throughout (*18*). The weighted average total energy of the quenched state is 1.9 times the weighted average ground-state energy in the deeper trap. Over the first two cycles, the shapes of all the distributions are self-similar (Fig. 2B, insets). Figure 2B shows the evolution of the integrated energy associated with the rapidities, which is the total energy minus the trap potential energy (*17*). The squares are for the experiment (fig. S4), the dashed line shows the theory for an average number of atoms, and the circles show the theory using the measured number of atoms at each point (*17*). After the quench, the calculated average cloud size drops from 14 μm to 3 μm, and $\bar{\gamma}$ drops from 1.4 to 0.3 (fig. S5, A to J). Figure 2 clearly shows that GHD accurately describes these experiments, where the weighted average (maximum) number of atoms per 1D gas is 60 (140) and the nature of the quasiparticles changes gradually during the collapse. The onset of multiple Fermi seas for this setup occurs in the third cycle. By the 11th cycle, we experimentally observe a loss of self-similarity that is consistent with our theoretical calculations. However, by that time, an ~20% atom loss complicates the theory beyond the scope of this work (*19*) (fig. S6).

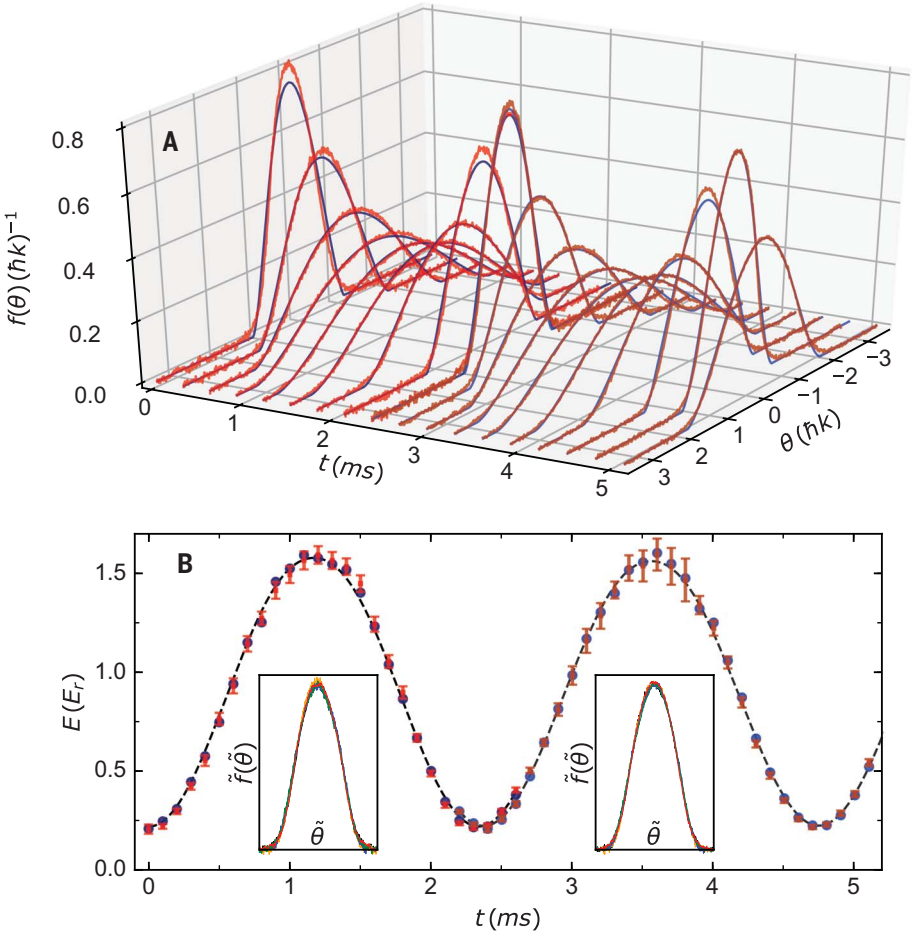

Fig. 2. Intermediate coupling (10-fold) trap quench. (**A**) Time evolution of the rapidity distribution after the trap is suddenly made 10 times deeper for 1D gases with $\bar{\gamma}_0 = 1.4$. The red curves show the experimental rapidity distributions over the course of the first two collapse cycles. The blue curves are the associated GHD theory, taking into account the measured atom number at each point (fig. S2, A and B). The slight difference in color for the two cycles denotes a 2.7% change in the trap depth associated with the slow experimental drift (*17*). (**B**) Time evolution of the rapidity energy, *E*, after the quench. The red squares are extracted from experimental distributions like those in (A) (*17*). The blue circles are for the associated GHD theory. The dashed line is the GHD theory for the average atom number. The two insets show the rescaled (to the same height and area) experimental rapidity distributions ($\tilde{f}$ versus $\tilde{\theta}$, with arbitrary units) for points throughout the first and second cycles, respectively (0, π/4, π/2, 3π/4, and π phase points are black, orange, blue, green, and red, respectively). The curves are shape invariant.

With $\bar{\gamma}_0 = 9.3$ we can measure dozens of cycles without appreciable loss and can quench to a 100-times-deeper trap. In this case, the weighted average total energy of the quenched state is 7.3 times the weighted average ground-state energy in the deeper trap. Figure 3A shows the rapidity evolution over the first two cycles. The shapes are no longer self-similar by the end of the first cycle (Fig. 3B, insets). The GHD theory agrees well with the experiment throughout. A second Fermi sea (Fig. 1C) emerges during the first collapse; GHD is essential past that point. Figure S5K shows theoretical calculations of the evolution of cloud sizes; averaged over all 1D gases, the full width at half the central density decreases by a factor of 35, from 17.5 μm to 0.5 μm. Although the cloud size of the central 1D gases remains similar to the average, sharp features appear that are suppressed by averaging. Similar sharp features appear in the rapidity distributions of single 1D gases, and these also tend to be suppressed by averaging (figs. S7 and S8).

The squares, the dashed line, and the circles in Fig. 3B show the integrated rapidity energy as a function of time for, respectively, the experiment (fig. S4), the theory with the average atom number, and the theory with the measured atom numbers (fig. S9). The squares in Fig. 3C show the integrated kinetic energy as a function of time, determined from the measured momentum distributions. The momentum measurement near peak compression is somewhat compromised by the large interaction energy, some of which gets converted to kinetic energy early in the time of flight. There is no corresponding complication in the rapidity measurement. We extract the theoretical kinetic energy from GHD by using the Lieb-Liniger model in each GHD spatial cell to determine the interaction energy, integrating it and subtracting it from the total integrated rapidity energy (*17*). We adjust the axial trap depth in the theory to account for day-to-day experimental drifts (<4%). The dashed line in

Fig. 3C shows the result for the average atom number; the circles use the measured atom numbers. Figure 3D shows the difference between the rapidity and kinetic energies as a function of time, both experimentally and theoretically (with measured atom numbers), and the inset shows the theory for a fixed atom number and trap depth.

The data in Fig. 3 test the range of validity of GHD in two distinct ways. First, the weighted average (maximum) occupancy in the 1D gases is 11 (25), challenging the continuum approximation. To gain confidence in this surprising result, we have compared GHD in the infinite γ limit with exact theory, which is only available in that regime (*17*). There are short wavelength features (Friedel-like oscillations) in the exact calculations for single 1D gases. For our distribution of 1D gases with different atom numbers, these features are smoothed out and the GHD theory overlaps the exact one (fig. S7). Second, during the compression, $\bar{\gamma}$ drops from 9.3 to 0.4 (fig. S5M), with the final factor-of-8 decrease occurring in the final 0.2 ms (right after the kinetic energy maximum). During this time, the ratio of interaction energy to kinetic energy increases from 0.076 to 4.2, as illustrated by the first peak in Fig. 3D. The momentum distributions in this final stage of compression change shape from fermionic to bosonic, as was shown in (*5*) using a less drastic quench. Our results validate the GHD description even in the face of rapid variations in the nature of the quasiparticles, suggesting that the system remains locally equilibrated to the GGE throughout.

We next study rapidity distributions during the sixth oscillation cycle (Fig. 4, A to F, and fig. S8). The theoretical distributions now change more noticeably during the cycle. Their distinctive shapes match the experimental curves reasonably well, except for slight experimental asymmetries caused by drifts in the gravity-canceling vertical magnetic field gradient, which lead to initial displacements of atoms from the light trap center by up to 100 nm, or 0.006 of the full width of their distribution (*17*). By the 11th cycle, finer features appear in the theory that are smeared out in the experiment (fig. S10, A to D), presumably on account of the initial atom cloud displacements and perhaps light trap asymmetry. In Fig. 4G, we show the integrated rapidity energies for cycles up to the 21st for the experiment and theory, with the period adjusted to account for small trap depth drifts (see fig. S10, E to I, for the corresponding rapidity distributions). The theory shows that there is $\lesssim$20% loss of contrast in individual 1D gases, with the additional contrast loss coming from the inhomogeneity of axial trap depths. An extensive quantity, the rapidity energy is less sensitive to minor experimental imperfections. GHD is accurate enough to describe these

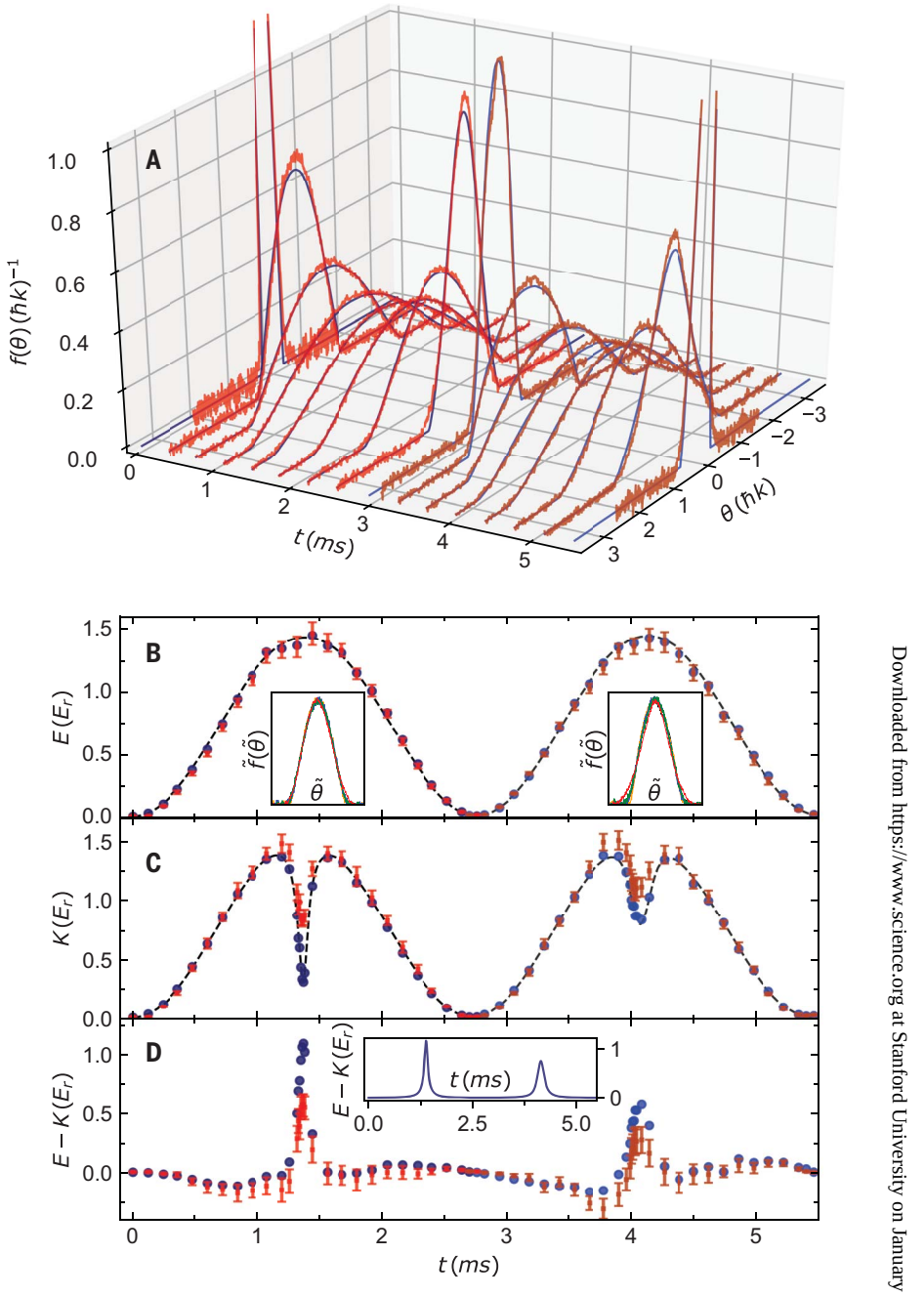

Fig. 3. Strong coupling (100-fold) trap quench. (**A**) Time evolution of the rapidity distribution after the trap is suddenly made 100 times deeper for 1D gases with $\bar{\gamma}_0$ = 9.3. The red curves show the experimental rapidity distributions over the course of the first two collapse cycles. The blue curves are the associated GHD theory, accounting for the measured atom number at each point (fig. S2, C and D). The slight difference in color for the two cycles denotes a 1% change in the trap depth due to the slow experimental drift (*17*). (**B**) Time evolution of the rapidity energy, E, after the quench. The red squares are extracted from experimental distributions like those in (A) (*17*). The blue circles are for the associated GHD theory. The dashed line is the GHD theory using the average atom number. The two insets show the rescaled (to the same height and area) experimental rapidity distributions for points throughout the first and second cycles, respectively (points near 0, $\pi/4$, $\pi/2$, $3\pi/4$, and π phases are shown in black, orange, blue, green, and red, respectively). By the second cycle, the distributions are no longer self-similar. (**C**) Time evolution of the kinetic energy, K, after the quench, measured from the momentum distribution just as the rapidity energy is measured from the rapidity distribution. The labeling is the same as for (B), but the trap depths are slightly (<4%) different (see fig. S2, E and F, for the associated atom numbers). (**D**) Time evolution of the interaction energy after the quench. The experimental and GHD theory points are obtained from (B) and (C) by subtracting K from E at each time. The inset shows GHD theory for a constant atom number and trap depth.

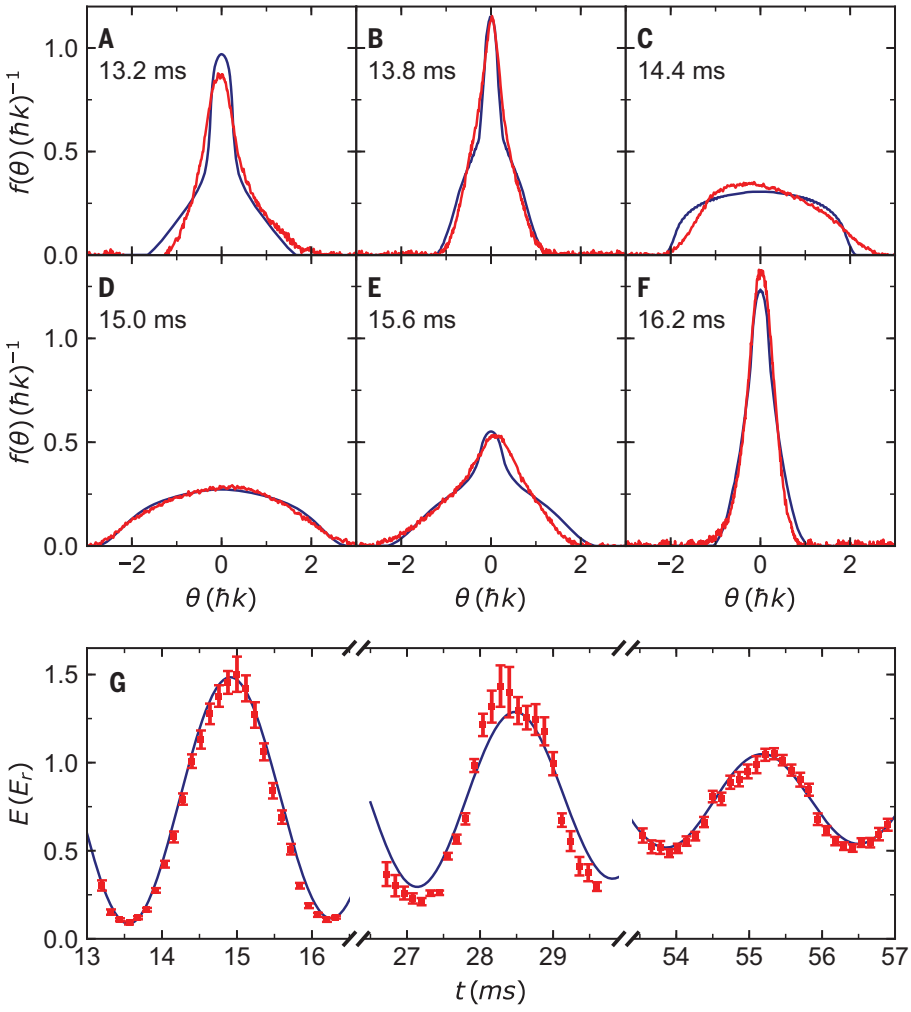

Fig. 4. Strong coupling (100-fold) trap quench at long times. (**A** to **F**) Experimental and GHD theory rapidity distributions during the sixth cycle after the 100-fold quench. The red curves show the experiment, the blue curves the associated theory. (**G**) The rapidity energy during the 6th, 11th, and 21st oscillations after the quench. For all the theory curves in this figure, we use the average number of atoms for each cycle, and the trap depth has been adjusted for each cycle so that the theory is in phase with the experiment.

experiments for the available measurement times.

We have shown that GHD accurately describes the dynamics of nearly integrable 1D Bose gases, with strong and intermediate coupling, after a trap quench. We experimentally challenged GHD's two underlying assumptions, the continuum and local GGE approximations, and we did so for long evolution times. A natural next step would be to study arrays of identical 1D gases or to further study single 1D gases, where it might be possible to observe finer features in rapidity distributions and to see direct evidence of the presence of multiple Fermi seas. One could also explore GHD in spin chains (*20*) and perform similar tests on systems that are further from integrable (*21*), for example, because of dipolar interactions in 1D gases (*22*) or dimensional crossover from 1D to 3D, a regime for which extensions to GHD have been recently explored (*23*). Looking ahead, GHD and its extensions promise to become a standard tool in the description of strongly interacting 1D quantum dynamics close to integrable points. Such points describe a wide range of experiments involving 1D ultracold gases of bosons (*24*) and fermions (*25*), as demonstrated in experiments in continuum (*26*–*28*) and lattice (*29*–*31*) systems.

REFERENCES AND NOTES

1. H. Bethe, *Z. Phys.* **71**, 205–226 (1931).
2. J.-S. Caux, F. H. L. Essler, *Phys. Rev. Lett.* **110**, 257203 (2013).
3. O. A. Castro-Alvaredo, B. Doyon, T. Yoshimura, *Phys. Rev. X* **6**, 041065 (2016).
4. B. Bertini, M. Collura, J. De Nardis, M. Fagotti, *Phys. Rev. Lett.* **117**, 207201 (2016).
5. J. M. Wilson *et al.*, *Science* **367**, 1461–1464 (2020).
6. B. Doyon, *SciPost Phys. Lect. Notes* 18 (2020).
7. M. Rigol, V. Dunjko, V. Yurovsky, M. Olshanii, *Phys. Rev. Lett.* **98**, 050405 (2007).
8. M. Schemmer, I. Bouchoule, B. Doyon, J. Dubail, *Phys. Rev. Lett.* **122**, 090601 (2019).
9. E. H. Lieb, W. Liniger, *Phys. Rev.* **130**, 1605–1616 (1963).
10. G. De Rosi, S. Stringari, *Phys. Rev. A* **94**, 063605 (2016).
11. S. Peotta, M. D. Ventra, *Phys. Rev. A* **89**, 013621 (2014).
12. B. Doyon, J. Dubail, R. Konik, T. Yoshimura, *Phys. Rev. Lett.* **119**, 195301 (2017).
13. J.-S. Caux, B. Doyon, J. Dubail, R. Konik, T. Yoshimura, *SciPost Phys.* **6**, 070 (2019).
14. T. Fokkema, I. S. Eliëns, J.-S. Caux, *Phys. Rev. A* **89**, 033637 (2014).
15. J.-S. Caux, R. M. Konik, *Phys. Rev. Lett.* **109**, 175301 (2012).
16. T. Kinoshita, T. Wenger, D. S. Weiss, *Science* **305**, 1125–1128 (2004).
17. See supplementary materials.
18. J.-F. Riou, L. A. Zundel, A. Reinhard, D. S. Weiss, *Phys. Rev. A* **90**, 033401 (2014).
19. I. Bouchoule, B. Doyon, J. Dubail, *SciPost Phys.* **9**, 044 (2020).
20. P. N. Jepsen *et al.*, *Nature* **588**, 403–407 (2020).
21. A. J. Friedman, S. Gopalakrishnan, R. Vasseur, *Phys. Rev. B* **101**, 180302 (2020).
22. Y. Tang *et al.*, *Phys. Rev. X* **8**, 021030 (2018).
23. F. Møller *et al.*, *Phys. Rev. Lett.* **126**, 090602 (2021).
24. M. A. Cazalilla, R. Citro, T. Giamarchi, E. Orignac, M. Rigol, *Rev. Mod. Phys.* **83**, 1405–1466 (2011).
25. X.-W. Guan, M. T. Batchelor, C. Lee, *Rev. Mod. Phys.* **85**, 1633–1691 (2013).
26. T. Kinoshita, T. Wenger, D. S. Weiss, *Nature* **440**, 900–903 (2006).
27. G. Pagano *et al.*, *Nat. Phys.* **10**, 198–201 (2014).
28. W. Kao, K.-Y. Li, K.-Y. Lin, S. Gopalakrishnan, B. L. Lev, *Science* **371**, 296–300 (2021).
29. B. Paredes *et al.*, *Nature* **429**, 277–281 (2004).
30. T. Fukuhara *et al.*, *Nature* **502**, 76–79 (2013).
31. M. Boll *et al.*, *Science* **353**, 1257–1260 (2016).
32. D. Weiss, N. Malvania, Y. Zhang, Y. Le, M. Rigol, Replication Data for: Generalized hydrodynamics in strongly interacting 1D Bose gases, Version 1, Harvard Dataverse (2021); https://doi.org/10.7910/dvn/xyxmyb.
33. J. Dubail, jdubail/Zero-entropy-GHD: Example of zero-entropy GHD simulation: quasi-harmonic trap quench in the one-dimensional Bose gas, Version 1, Zenodo (2021); https://doi.org/10.5281/zenodo.5094916.

ACKNOWLEDGMENTS

Funding: Supported by NSF grants PHY-2012039 (D.S.W., N.M., and Y.L.) and PHY-2012145 (Y.Z. and M.R.), and by US Army Research Office grant W911NF-16-0031-P00005 (D.S.W., N.M., and Y.L.). The computations were carried out at the Institute for Computational and Data Sciences at Penn State. **Author contributions:** N.M. and Y.L. carried out the experiments. Y.Z. carried out the theoretical calculations. D.S.W. oversaw the experimental work. J.D. and M.R. oversaw the theoretical work. All authors were involved in the analysis of the results, and all contributed to writing the paper. **Competing interests:** There are no conflicts of interests. **Data and materials availability:** The presented data (*32*) and the core theoretical code (*33*) are archived.

SUPPLEMENTARY MATERIALS

science.sciencemag.org/content/373/6559/1129/suppl/DC1
Materials and Methods
Supplementary Text
Figs. S1 to S10
References (*34*–*50*)

29 September 2020; accepted 2 August 2021
10.1126/science.abf0147

Generalized hydrodynamics in strongly interacting 1D Bose gases

Neel MalvaniaYicheng ZhangYuan LeJerome DubailMarcos RigolDavid S. Weiss

Science, 373 (6559), • DOI: 10.1126/science.abf0147

Monitoring quantum dynamics

Reducing the dimensionality of a quantum system of interacting particles can simplify its physics. Such reduction is possible in ultracold atomic gases, where a lattice of one-dimensional (1D) gases can be generated using optical potentials. Malvania *et al*. studied the dynamics of 1D rubidium-87 atomic gases after a sudden increase in the axial trapping potential. Normally, these dynamics would be difficult to describe theoretically, but the researchers found that a theory called generalized hydrodynamics captured the behavior of their 1D system over a long time evolution. —JS